Neuron, Vol. 19, 1249–1259, December, 1997, Copyright ©1997 by Cell Press

In Vivo Analysis of the Drosophila Light-Sensitive Channels, TRP and TRPL

Helmut Reuss, Mart H. Mojet,*
Sylwester Chyb, and Roger C. Hardie†
Department of Anatomy
Cambridge University
Cambridge CB2 3DY
United Kingdom

Summary

We have tested the proposal that the light-sensitive conductance in Drosophila is composed of two independent components by comparing the wild-type conductance with that in mutants lacking one or the other of the putative light-sensitive channel subunits, TRP and TRPL. For a wide range of cations, ionic permeability ratios in wild type were always intermediate between those of *trp* and *trpl* mutants. Effective channel conductances derived by noise analysis in wild type were again intermediate (17 pS; c.f. 35 pS in *trp* and 4 pS in *trpl*) and also showed a complex voltage dependence, which was quantitatively explained by the summation of TRPL and TRP channels after taking their different reversal potentials into account. Although La^{3+} partially blocked the light response in wild-type photoreceptors, it increased the effective single channel conductance. The results indicate that the wild-type light-activated conductance is composed of two separate channels, with the properties of TRP- and TRPL-dependent channels as determined in the respective mutants.

Introduction

Phototransduction in Drosophila is mediated by a G protein–coupled phosphoinositide (PI) cascade culminating in the opening of calcium- and cation-selective channels in the plasma membrane (reviewed by Hardie and Minke, 1995; Ranganathan et al., 1995; Zuker, 1996). Evidence summarized below suggests that these light-sensitive channels are encoded at least in part by the transient receptor potential (*trp*) gene (Cosens and Manning, 1969; Minke et al., 1975; Montell and Rubin, 1989) and its homolog, *trp*-like (*trpl*; Phillips et al., 1992). The *trp* gene is the prototypical member of a novel ion channel family within the superfamily of voltage-gated and cyclic nucleotide–gated channels, its structure suggesting that it encodes one subunit of a multimeric channel assembly (reviewed by Hardie and Minke, 1993; Hardie, 1996a; Minke and Selinger, 1996). Significantly, recently discovered vertebrate and human homologs of *trp* have been implicated in the widespread but poorly understood phenomenon of PI-regulated Ca^{2+} entry, often referred to as store-operated or capacitative Ca^{2+} entry (Wes et al., 1995; Zhu et al., 1996; Zitt et al., 1996; reviewed by Clapham, 1996).

The identification of TRP and TRPL as PI-regulated Ca^{2+} influx channels stems from genetic analysis in Drosophila. Mutations in the transient receptor (*trp*) gene greatly reduce the Ca^{2+} selectivity of the light-sensitive current (Hardie and Minke, 1992). The remaining current in the *trp* mutant appears to be mediated by a nonselective cation channel with significant permeability to Ca^{2+} and is largely abolished by a null mutation of the *trpl* gene (i.e., in a *trp;trpl* double mutant; Niemeyer et al., 1996). These results have led to the suggestion that the light-sensitive conductance in Drosophila is composed of two independent components: one encoded by the *trp* gene, and the other encoded by *trpl*. Heterologous expression of TRP and TRPL in Xenopus oocytes (Petersen et al., 1995; Gillo et al., 1996; Lan et al., 1996) and insect cell lines (Vaca et al., 1994; Harteneck et al., 1995; Hardie et al., 1997) add some support to this proposal, since TRP expression is reported to generate a Ca^{2+}-selective conductance, whereas TRPL generates a nonselective cationic conductance. However, Gillo et al. (1996) and Xu et al. (1997) recently reported evidence suggesting heteromultimeric subunit assembly of TRP and TRPL subunits. The present study was designed to examine more critically whether the in situ wild-type light-sensitive conductance can indeed be considered as the sum of two components, and if so, whether these correspond to TRP and TRPL or whether there is a de novo conductance indicative of heteromultimeric assembly. To address this question, which has implications not only for the structure of this novel ion channel family but also for possible mechanisms of activation and regulation, we have compared a variety of properties of the wild-type conductance with those of the TRPL- and TRP-dependent channels isolated in the respective mutants, *trp* and *trpl*. Our results support the hypothesis that TRP and TRPL channels operate as distinct entities in wild-type flies. Furthermore, our measurements in *trpl* represent the first detailed descriptions of the TRP-dependent conductance in situ, thereby allowing a revealing comparison with the properties of heterologously expressed TRP channels (e.g., Vaca et al., 1994; Xu et al., 1997).

Results

Reversal Potentials and Ionic Selectivity

Reversal potentials (E_{rev}) were measured under a variety of ionic conditions by recording responses to brief light flashes as the membrane potential was stepped in small (2, 5, or 10 mV) steps around E_{rev}. When bathed in normal physiological Ringer's solutions (120 mM NaCl, 5 mM KCl, 1.5 mM Ca^{2+}, and 4 mM Mg^{2+}), E_{rev} in *trpl* photoreceptors (11.6 ± 0.9 mV [mean ± SD]; n = 11) showed a small but statistically highly significant ($p < 0.0001$, Student's t test) positive shift compared to wild type (9.2 ± 1.4 mV; n = 22). As previously reported, E_{rev} in trp^{301} (−4.3 ± 1.1 mV; n = 8) showed a large negative

*Present address: Department of Physiology, University College London, Gower Street, London WC1E 6BT, United Kingdom.
†To whom correspondence should be addressed.

shift with respect to wild type (Hardie and Minke, 1992; Niemeyer et al., 1996).

Previous estimates of the ionic permeabilities of the light-sensitive channels in Drosophila were made in the presence of several ionic species using the Goldman Hodgkin Katz (GHK) equations (Hardie and Minke, 1992). In order to gain more reliable estimates of both monovalent and divalent ionic permeability ratios, reversal potentials were determined under bi-ionic conditions in which Cs^+ was the only cation included in the pipette solution, whereas the bath contained only one of a variety of monovalent or divalent cations. Under these conditions, permeability (P) ratios can be derived from the bi-ionic reversal potential (E_{rev}) according to:

$$P_M:P_{Cs} = \frac{[Cs_i].\ e^{E_{rev}/(RT/F)}}{[M_o]} \quad \text{[Equation 1 for monovalent ions]}$$

$$P_D:P_{Cs} = \frac{[Cs_i].\ e^{E_{rev}/(RT/F)}}{4.[D_o]} \quad \text{[Equation 2 for divalent ions, e.g., Hille, 1992]}$$

For monovalent species, the bath contained equimolar concentrations of the respective ionic species (Na^+ or Li^+). K^+ was not tested because the large voltage-sensitive K^+ conductances in Drosophila photoreceptors make accurate measurements impractical. The results (Figure 1; Table 1) broadly confirm previous results using multi-ion solutions, showing that the light-sensitive conductance in wild-type flies has a greater permeability for Na^+ ($P_{Na}:P_{Cs} = 1.16$), whereas in *trp* mutants Cs^+ is significantly more permeable ($P_{Na}:P_{Cs} = 0.84$). In *trpl* mutants, there is a slight positive shift in E_{rev} of ~2–3 mV indicative of an even higher Na^+ permeability. By contrast, wild-type, *trp*, and *trpl* flies all appear to have roughly the same relative permeability for Li^+ ($P_{Li}:P_{Cs}$ in range 0.8–0.9).

For divalent ion species, external concentrations of 10 mM were used in combination with 120 mM N-methyl-D-glucamine ($NMDG^+$), which appears to be essentially impermeant, as no inward currents can be measured when $NMDG^+$ is the only external cation (Hardie and Minke, 1992). However, when Ca^{2+} was the only permeant external cation we found it virtually impossible to record responses to light, probably because Na/Ca exchange no longer operates and the cells rapidly become loaded with damaging levels of Ca^{2+}. We therefore used a strategy of first recording in a bath solution containing only NMDG Cl, using a pipette solution containing 130 mM Cs gluconate, 10 mM EGTA, and 1 mM $CaCl_2$. Only after establishing the whole-cell configuration (thereby buffering internal Ca^{2+} with EGTA) was the test solution containing 10 mM Ca^{2+} and 120 mM NDMG applied to the cell by puffer pipette, and reversal potential measurements were performed (e.g., Gomez and Nasi, 1996). Although not strictly necessary, other divalent cations were tested in exactly the same way.

With 10 mM [Ca_o] and 130 mM [Cs_i], E_{rev} in wild-type flies was 32.7 ± 3.3 mV (n = 6; Figure 1), indicating that $P_{Ca}:P_{Cs}$ equaled 45:1, which agrees well with previous measurements based on Ca^{2+}-dependent shifts in E_{rev} in the presence of a variety of other internal and external cations (Hardie and Minke, 1992). When external [Ca_o] was reduced 10-fold (to 1 mM), E_{rev} shifted to 6.9 ± 2.3 mV (n = 7), i.e., by ~26 mV, which is close to the Nernst prediction (29 mV). Similar measurements in the *trp* mutant directly confirm the much-reduced Ca^{2+} permeability (Hardie and Minke, 1992). However, in the *trpl* mutant, E_{rev} was ~10 mV more positive than in wild type, indicating that the Ca^{2+} selectivity of the TRP-dependent channels was significantly greater ($P_{Ca}:P_{Cs}$ = ~110:1). Although these channels are less selective than, for example, voltage-sensitive Ca^{2+} channels or calcium release–activated current (I_{CRAC}; Hoth and Penner, 1993), these data demonstrate the high Ca^{2+} selectivity of TRP-dependent channels in situ.

Figure 1 and Table 1 summarize results measured for a variety of monovalent and divalent cations, including

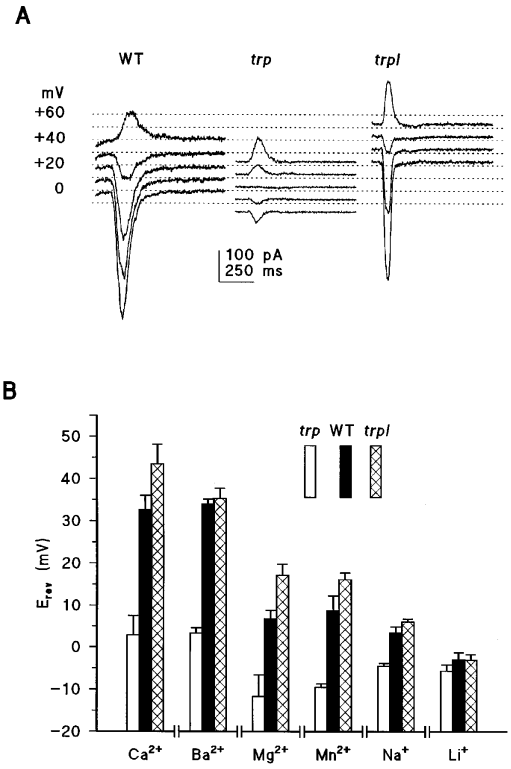

Figure 1. Bi-ionic Reversal Potentials

(A) Reversal potentials determined under bi-ionic conditions with 10 mM external Ca^{2+} and 130 mM internal Cs^+ in wild-type, trp^{301}, and *trpl* photoreceptors. Responses to 50 ms flashes were recorded as the holding potential was stepped in 10 mV intervals as indicated (wild type from −2 to 38 mV; *trp* from −17 to 23 mV, and *trpl* from 23 to 53 mV; values corrected for −12 mV junction potential). In order to restrict the damaging effects of Ca^{2+} influx in the absence of Na/Ca exchange, the test solution (10 mM $CaCl_2$, 120 mM NMDG Cl) was applied by puffer pipette after initially bathing the cells in 130 mM NMDG Cl. In addition to 130 mM Cs gluconate, the pipette solution contained 10 mM EGTA and 1 mM $CaCl_2$ to buffer Ca^{2+} influx.

(B) Summary of reversal potentials recorded under a variety of bi-ionic conditions. With the exception of Li^+, for which values are not statistically separable, E_{rev} in wild type always fell between that of *trp* and *trpl*. The permeability ratios in Table 1 were derived from these data using Equations 1 and 2. Error bars are standard deviations; the data are based on at least 4 cells for each measurement (see Table 1).

Table 1. Ionic Permeability Ratios of TRP- and TRPL-Dependent Conductances

	P_{TRP} (in *trpl*)	P_{TRPL} (in *trp*)	P_{WT}	% TRPL
$P_{Ca}:P_{Cs}$	109.9 ± 44.3 (6)	4.3 ± 1.6 (7)	45.1 ± 11.6 (6)	61 ± 11
$P_{Ba}:P_{Cs}$	54.8 ± 12.3 (6)	4.2 ± 0.5 (6)	48.9 ± 4.3 (6)	12 ± 9
$P_{Mg}:P_{Cs}$	13.0 ± 2.9 (6)	1.4 ± 0.6 (6)	5.7 ± 0.8 (5)	63 ± 6
$P_{Mn}:P_{Cs}$	11.8 ± 1.5 (6)	1.5 ± 0.1 (6)	6.8 ± 1.9 (6)	49 ± 18
$P_{Na}:P_{Cs}$	1.27 ± 0.06 (4)	0.84 ± 0.02 (4)	1.16 ± 0.06 (5)	26 ± 14
$P_{Li}:P_{Cs}$	0.89 ± 0.05 (8)	0.80 ± 0.05 (8)	0.89 ± 09 (7)	–

Permeability ratios ($P_x:P_{Cs}$) were derived from bi-ionic reversal potential data (Figure 1) using Equations 1 and 2. Data are expressed as mean ± SD (number of cells) with respect to internal Cs gluconate (130 mM). Divalents were measured using 10 mM external cations; monovalents, using 130 mM. No corrections were made for ionic activities. Channels were measured in respective mutants, i.e., TRPL channels were measured in the *trp* mutant, TRP-dependent channels were measured in *trpl*. The final column gives the percentage of the wild-type conductance that can be attributed to TRPL channels, assuming the wild-type conductance is the weighted sum of TRP and TRPL permeabilities as determined in the respective mutants (i.e., $P_{WT} = k \times P_{TRPL} + [1-k]P_{TRP}$). SD, in this case, was based on the SD of the wild-type permeability. For the case of Li^+, reversal potentials were not statistically separable (within 2–3 mV), making this derivation unreliable.

Na^+, Li^+, Ca^{2+}, Ba^{2+}, Mg^{2+}, and Mn^{2+}. In general, the wild-type value is intermediate between that of the *trp* and *trpl* mutants, as predicted if the wild-type current is the sum of independent TRP and TRPL components. On this assumption, the data allow direct estimates of the relative contributions of each conductance to the wild-type response under the various conditions (final column of Table 1; see Discussion).

Current–Voltage (I–V) Relationships

Under divalent-free conditions, I–V relationships of the light-activated conductance in both wild type and *trp* show a simple outward rectification, indicative of a voltage-dependent increase in channel open probability at depolarized potentials. In the presence of external Mg^{2+}, the wild-type I–V relationship develops a dual inward and outward rectification due to a voltage-dependent block by Mg^{2+}, which can be relieved by both hyperpolarization and depolarization (Hardie and Mojet, 1995). Mg^{2+} also blocks the current carried by TRPL channels isolated in the *trp* mutant, but to a lesser extent and with little if any voltage dependence, so that the I–V relationship retains a simple outward rectification (Figure 2; Hardie et al., 1997). In contrast, as shown in Figure 2, the I–V relationship of the light-sensitive conductance in the *trpl* mutant is similar to that of wild type in always showing a pronounced dual rectification, indicating that this property of the light-sensitive conductance does not require TRPL channels. A more precise comparison was not made, as the exact shapes of the I–V functions in wild type and *trpl* were found to be rather variable.

Biphasic Reversal Potential

When external Ca^{2+} is lowered to 0.5 mM in otherwise normal physiological Ringer's, adult wild-type photoreceptors show a "biphasic reversal potential"; i.e., there is no unique reversal potential, but at holding potentials close to reversal potential the light-induced current (LIC) is initially outward and then inward (e.g., Figure 3). This behavior has been interpreted as due to the sequential activation of two classes of channel with different reversal potentials (Hardie and Minke, 1992), which can be tentatively attributed to TRPL and TRP. However, in principle, a number of alternative explanations might also account for such biphasic behavior: (1) changes in ionic concentration gradients during the response; (2) imperfect space-clamp conditions, which would vary dynamically with the magnitude of the current; and (3) contribution of electrogenic Na/Ca exchange current to the response.

In order to obtain a quantitative measure for the biphasic behavior, we estimated E_{rev} during the early rising phase of the response and also during the late falling phase (responses averaged at times before 50% rise and after 50% decay; see Figure 3). The absolute difference (E_{BIP} in mV) was taken as an objective index of the biphasic behavior. Possibilities 1 and 2 above would predict that the biphasic behavior would become more pronounced with larger currents generated by higher intensities; however, Figure 3B shows that over a 6-fold range of intensity, whereby conductances increased by over 3-fold, E_{BIP} showed no significant difference. To test the possibility of Na/Ca exchange contributing to the waveform, we rapidly replaced external Na^+ with Cs^+ to block the exchanger, using a puffer pipette. The

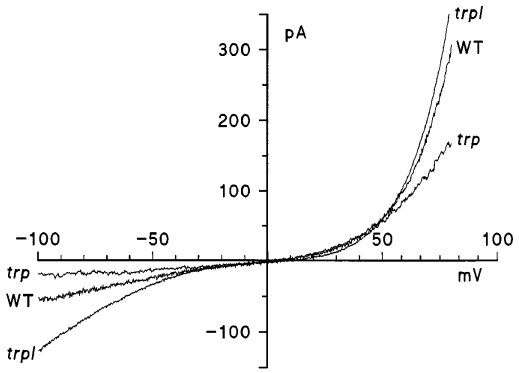

Figure 2. Current–Voltage (I–V) Relationships Determined from Voltage Ramps in Wild-Type, *trp*^{301}, and *trpl* Photoreceptors in Physiological Ringer's Containing 0 Ca^{2+} and 4 mM Mg^{2+}

The current in *trp* shows a simple exponential outward rectification; however, in both wild-type and *trpl* flies there is a conspicuous S-shaped inward and outward rectification under both conditions. Apart from a slight shift in reversal potential, no significant differences could be detected between I–V relationships of wild-type and *trpl* photoreceptors; however, there was considerable variation in the extent of the inward rectification in both cases, making precise comparison impossible. I–V relationships were derived using ramps from −100 to 80 mV applied during steady state light responses, subtracting a template recorded immediately before in the dark.

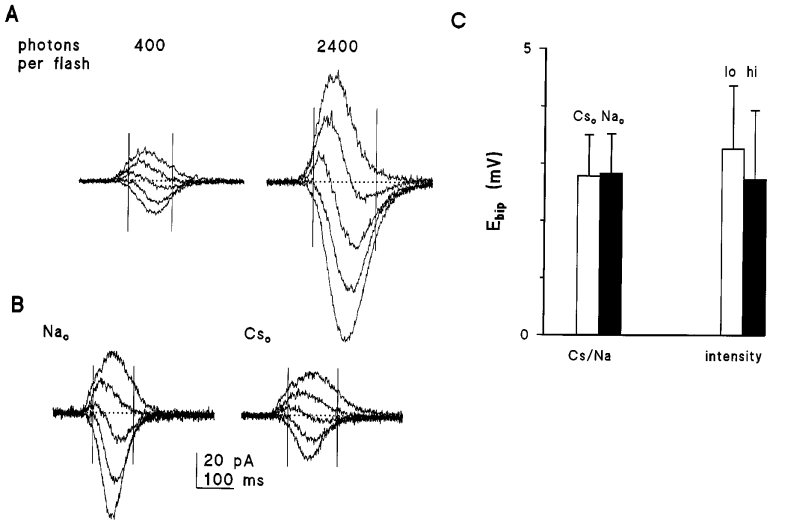

Figure 3. Biphasic Reversal Potential in Wild-Type Photoreceptors

(A and B) Families of responses to 20 ms flashes in wild-type photoreceptor in 2 mV steps around reversal potential (2–10 mV) showing biphasic responses near reversal potential. Increasing the intensity from 400 (lo) to 2400 (hi) photons per flash (A) or replacing external Na^+ with Cs^+ by puffer pipette (B) did not noticeably influence the biphasic behavior, although the Cs^+ substitution resulted in a ~2–3 mV shift in reversal potential. (C) An objective index of this biphasic behavior was obtained by estimating E_{rev} both during the rising phase (data points averaged before 50% rise of the fastest response) of the response and the tail of the response (after 50% decay of the slowest response; see vertical lines in [A] and [B]). The difference (in mV) is defined as E_{BIP} and was independent of intensity or the presence of external Na^+. Data averaged from at least two repeated determinations in four or five cells for each case. Responses were recorded with a bath containing 0.5 mM Ca^{2+} and 4 mM Mg and with a Cs TEA electrode to eliminate K channel activity and ~75% series resistance compensation.

substitution of Cs^+ induced the expected small change in E_{rev} due to the difference in permeability for Na^+ versus Cs^+; however, E_{BIP} was not affected.

Finally, if the biphasic behavior is a consequence of sequential activation of TRP and TRPL channels, then clearly responses in *trpl* flies should no longer show biphasic behavior. However, if any of the three alternatives suggested above account for the behavior, there is no obvious reason why a biphasic behavior should not also be seen in *trpl*. In over 50 cells, we never detected any significant biphasic behavior in *trpl* (e.g., Figure 5). As previously reported, neither did we detect a biphasic response in *trp* mutants (Hardie and Minke, 1992).

Noise Analysis

It has thus far proved impossible to directly patch-clamp the light-sensitive channels in Drosophila because of their inaccessible location in the microvilli. However, with certain assumptions, the amplitude of single channel currents can be derived from recordings of macroscopic channel noise as the ratio of the variance to the mean current (Colquhoun and Hawkes, 1977). In order to extract the high frequency noise from response to flashes of light, we used nonstationary analysis, while recording in Ca^{2+}-free Ringer's to slow down the kinetics of transduction. Smooth functions were fitted to individual light responses and subtracted from the original trace to isolate the high frequency channel noise. Plots of variance against mean current determined from short overlapping segments of the response for such data were approximately linear, allowing the effective amplitude of the underlying single channel currents to be derived directly from the slope (variance/mean). Single channel conductances were then estimated by dividing by the EMF (holding potential $-$ E_{rev}) and corrected for the fraction of power estimated to have been filtered by the recording bandwidth (see Experimental Procedures). The estimated single channel conductance of TRP channels isolated in *trpl* flies was rather low (4 pS), whereas in *trp* flies, where the current is carried by TRPL channels, the estimated channel conductance was ~10× greater (35 pS). Values in wild type were intermediate, as would be expected if both channels contributed to the response (the effective conductance now being the weighted average of the two). Qualitatively, this relation can be seen directly in the original traces; there is very little channel noise visible in *trpl* responses, whereas high frequency channel noise can clearly be seen in the *trp* mutant and, to a lesser extent, in wild type (Figure 4).

The values above were determined at resting potential (−70 mV). For a response mediated by one class of channel, the single channel conductance would normally be expected to be independent of voltage; however, in wild-type photoreceptors, the hypothesis that there are two independent channels with different reversal potentials and different single channel conductances predicts a very specific and unusual voltage dependence of effective channel conductance at voltages near reversal potential. Namely, as the command potential approaches E_{rev} for the TRPL channels, the response should be dominated by the low conductance TRP channels, whereas when the command potential approaches E_{rev} for TRP, the responses should be dominated by high conductance TRPL channels. At reversal potential, the estimated conductance should approach infinity since the average mean current is zero but variance is finite, as TRP channels would be expected to be mediating outward currents, balanced by inward currents carried by TRPL channels. Qualitative confirmation of this prediction can be directly observed in representative traces recorded in 0.5 mM Ca^{2+} Ringer, i.e., the same conditions used for measurements of biphasic reversal potentials (Figure 5). At 0 mV (near TRPL E_{rev}), responses in wild type were virtually noise-free (similar to *trpl* mutant); however, similar sized responses at 10 mV (near TRP E_{rev}) showed clear channel noise (similar to *trp* mutant). The apparent single channel conductances derived from such data in *trp*, *trpl*, and wild type, all assuming a

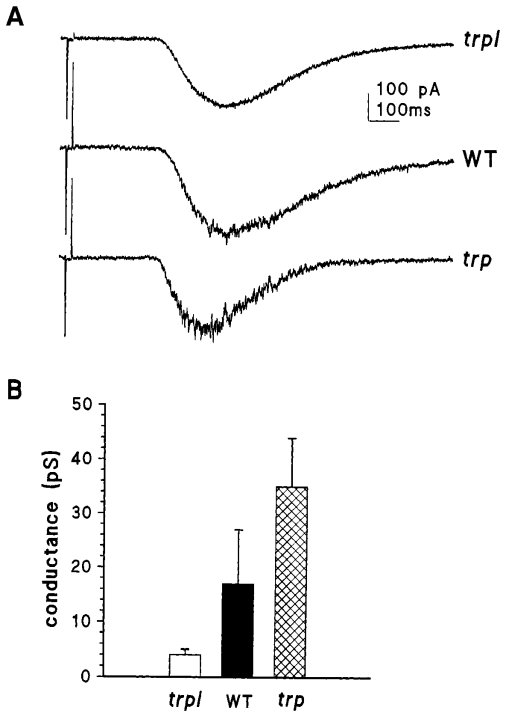

Figure 4. Channel Noise in Flash Responses Recorded at −70 mV in Ca^{2+}-Free Ringer's Solution in *trpl*, Wild Type, and *trp*.

(A) High frequency channel noise can be seen superimposed upon the response waveforms in all three cases, but differs in magnitude, being largest in *trp* and smallest in the *trpl* mutant. Before each flash, a −10 mV voltage step was delivered to measure the clamp time constant from exponential fits to the decay of the capacitative transient (no series resistance compensation applied).

(B) Effective channel conductances. Nonstationary noise analysis was used to extract the effective single channel currents (I = variance/mean) underlying the channel noise. Effective channel conductance (γ) was then calculated as γ = I/EMF (where EMF = holding potential − E_{rev}) and corrected for the power lost due to filtering by the recording bandwidth (see Experimental Procedures). The data, averaged from at least 10 flash responses in each cell, confirm that the effective conductance is low for TRP channels (in *trpl* mutant; n = 4 cells) and high for TRPL channels (in *trp*; n = 6), with intermediate values in wild type (n = 14).

single (measured) value for E_{rev}, are shown in Figure 5. As expected, in *trp* and *trpl*, values were independent of holding potential. However, in wild type the estimated conductance showed a characteristic dependence on voltage, which is accurately predicted by a simple arithmetic model based on the summation of the contributions of TRP and TRPL channels (solid line). In particular, there was a minimum of conductance at E_{rev} of the TRPL channels and a ~10-fold higher conductance near E_{rev} for TRP, whereas near the measured reversal potential, the estimated conductance approaches infinity. Since E_{rev} and channel conductance for TRP and TRPL channels were estimated in the respective mutants under the same conditions, the only free parameter used for modeling this voltage dependence was the relative proportion of the current carried by each channel. A good fit to the data was obtained assuming equal current carried by each component.

La^{3+} Block

Micromolar concentrations of La^{3+} completely blocks TRP channels but leaves TRPL channels unaffected (Hochstrate, 1989; Suss-Toby et al., 1991; Hardie and Minke, 1992; Niemeyer et al., 1996). The different channel conductances of TRP and TRPL channels leads to another otherwise counterintuitive prediction of the two-channel model: namely, that during a La^{3+}-induced block of the light-induced current in wild-type photoreceptors, there should be a reduction in amplitude but an increase in the estimated channel conductance. Figure 6 shows responses before and immediately after application of La^{3+} (20 μM) by puffer pipette. In agreement with the prediction, following application of La^{3+} responses were significantly attenuated, but relative channel noise increased. Figure 6B confirms that the effective channel conductance, estimated from the variance-to-mean ratio, did indeed increase as the block developed. In confirmation of the findings of Niemeyer et al. (1996), La^{3+} completely blocked the light response in *trpl* flies. However, variance-to-mean ratios determined during partial blocks induced by low doses of La^{3+} remained constant and indicative of a low channel conductance (Figure 6).

TRP and TRPL Channels Are Differentially Regulated by Ca^{2+}

Thus far our results, which were obtained either under Ca^{2+}-free conditions or at potentials near reversal potential, suggest that the TRP and TRPL channels contribute approximately equally to the light-sensitive conductance. This raises the question of why *trpl* mutant and wild-type light responses appear indistinguishable under physiological conditions (Niemeyer et al., 1996). We suspected that this apparent contradiction might be explained by differential regulation of TRP and TRPL channels by Ca^{2+} influx, leading to a dominant contribution of TRP channels at resting potential with normal (1.5 mM) external Ca^{2+}. To test this idea, responses to dim flashes were recorded in the same cells in the presence and absence of extracellular Ca^{2+}, using a puffer pipette containing EGTA-buffered Ca^{2+}-free Ringer's to rapidly remove extracellular Ca^{2+}. As previously reported (Hardie, 1991), in wild-type flies, responses in the presence of extracellular Ca^{2+} are facilitated but inactivate more rapidly due to sequential positive and negative feedback mediated by Ca^{2+} influx (Figure 7). In *trpl* mutants, this behavior is even more pronounced, such that peak responses in the presence of Ca^{2+} are increased ~8-fold. In marked contrast, in *trp* mutants responses in the presence of Ca^{2+} inactivated more rapidly, whereas the rising phase was unaltered, and on average peak responses were reduced ~2.5-fold. Compared to Ca^{2+}-free conditions, therefore, these results predict that the relative contribution of TRPL channels to the wild-type light response should be reduced by ~20-fold at resting potential in the presence of physiological levels of Ca^{2+}.

The *trpl;trp^{CM}* Double Mutant Is Blind

Niemeyer et al. (1996) reported that sensitivity to light was substantially diminished but not abolished in a *trpl;trp^{301}* double mutant. Since the residual response was found to be blocked by La^{3+}, they suggested that

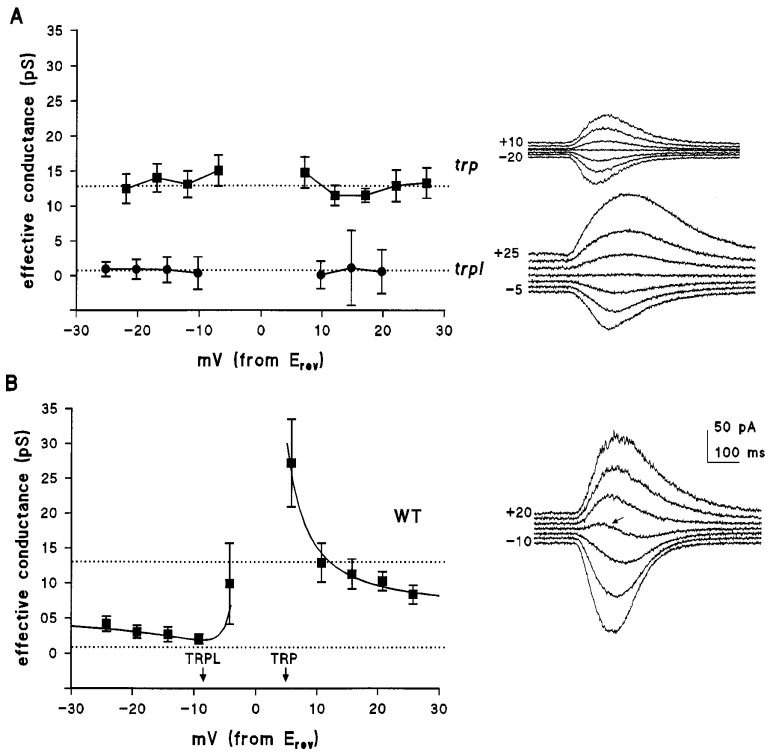

Figure 5. Voltage Dependence of Apparent Effective Conductance Calculated from High Frequency Channel Noise at Potentials near Reversal Potential (0 mV)

Nonstationary noise analysis was used to extract the effective single channel conductance, γ (see Figure 4 legend and Experimental Procedures).

(A) As expected for the case of a current carried by a single channel, in both *trp* and *trpl* flies the calculated channel conductance is independent of voltage; however, values differ ~10-fold (absolute values are smaller than in Figure 4, as they have not been corrected for filtering by the recording bandwidth).

(B) In wild type, the derived effective conductance shows a characteristic voltage dependence, reaching a minimum ~5–10 mV below the measured reversal potential, with ~10× larger values for outward currents. Near E_{rev}, values approach infinity as the mean current approaches zero, whereas variance is still finite (e.g., inset [wild type indicated by arrow]). The smooth curve is the behavior predicted by a simple arithmetic model assuming two channels with the single channel conductances and reversal potentials measured in the *trp* and *trpl* mutants, respectively, each contributing 50% of the macroscopic conductance. Data are averaged from five cells in each case; voltages are expressed with respect to reversal potential to facilitate comparison. The actual E_{rev} values measured under these conditions (0.5 mM Ca^{2+}, 4 mM Mg^{2+}) were 5.9 (wild type), 10.8 (*trpl*), and −2.9 mV (*trp*) mV. Arrows in (B) indicate E_{rev} of TRP- and TRPL-dependent channels. Insets (right) show examples of responses used to derive these data; each family of traces are responses to 20 ms flashes at a series of holding potentials in 5 mV steps around reversal potential (range indicated). Apart from the absolute shifts in reversal potential, note that (1) at reversal potential in wild type (arrow), there is a biphasic response (see also Figure 3), but both *trp* and *trpl* have a unique reversal potential; (2) in *trp*, a minimum in the high frequency channel noise is seen at reversal potential; however, in wild type, minimum variance is observed at a holding potential negative to E_{rev} (arrow shows clear high frequency channel noise at reversal potential); and (3) in *trp*, the noise bandwidth is similar for inward and outward currents; however, in wild type, more noise is associated with the outward currents. In *trpl* noise is uniformly low at all holding potentials.

trp^{301} was not a completely null allele and that the residual response was mediated by a small number of TRP channels. However, it is also possible that the residual response represents a further class of La^{3+}-sensitive light-sensitive channel. In an attempt to resolve this issue, we generated a *trpl;trp* double mutant using a different *trp* allele, *trp^{CM}*. This allele is a developmentally temperature-sensitive mutation that, when reared at 19°C, produces substantial amounts of functional TRP protein (Minke, 1983; Pollock et al., 1995); however, when raised at 25°C it appears to have a near null phenotype, indistinguishable from *trp^{301}*. Figure 8 shows responses in *trpl;trp^{CM}* flies elicited by a supersaturating stimulus from a high voltage Xe flash lamp, which in wild-type or *trpl* flies evoked responses in excess of 20 nA (not shown). The initial biphasic response is the early receptor current, which represents the charge movement due to rhodopsin photoisomerization (Pak and Liddington, 1974). This is of similar size to that measured in wild-type flies (Hardie, 1995) and demonstrates that the photoreceptors have a near normal complement of rhodopsin. Otherwise, there was virtually no other response to the flash (Figure 8). This profound loss of responsiveness to light in *trpl;trp^{CM}* was also confirmed using electroretinogram (erg) recordings, in which no response at all could be detected (n = 12). By contrast, in *trpl;trp^{301}* the same Xe flash stimulus elicited responses in excess of 500 pA (750 ± 138 pA; n = 5), whereas erg recordings showed robust responses with sensitivity reduced ~3–4 log units compared to wild type or *trpl* (data not shown). As a useful control against any effect of genetic background, when the same *trpl;trp^{CM}* stock was reared at the permissive temperature of 19°C, large (~4 nA) responses could be recorded in response to the Xe flash stimulus (Figure 8), whereas sensitivity determined using dimmer flashes was found to be reduced by only ~2–3 log units with respect to wild type or *trpl* (data not shown). These results thus indicate that loss of functional *trp* and *trpl* gene products leads to complete abolition of the light response and that, unlike *trp^{301}*, *trp^{CM}* is functionally a complete null allele when reared at 25°C, even though protein can still be detected with TRP antibodies (Pollock et al., 1995).

Discussion

We have investigated a variety of properties of the light-sensitive conductance in wild-type photoreceptors and compared these with the properties in *trp* and *trpl* mutants lacking one or the other of the two putative channel subunits, TRP and TRPL. The results are consistent with the hypothesis that TRP and TRPL contribute independently to the wild-type response and provide estimates of the relative contributions of each component under

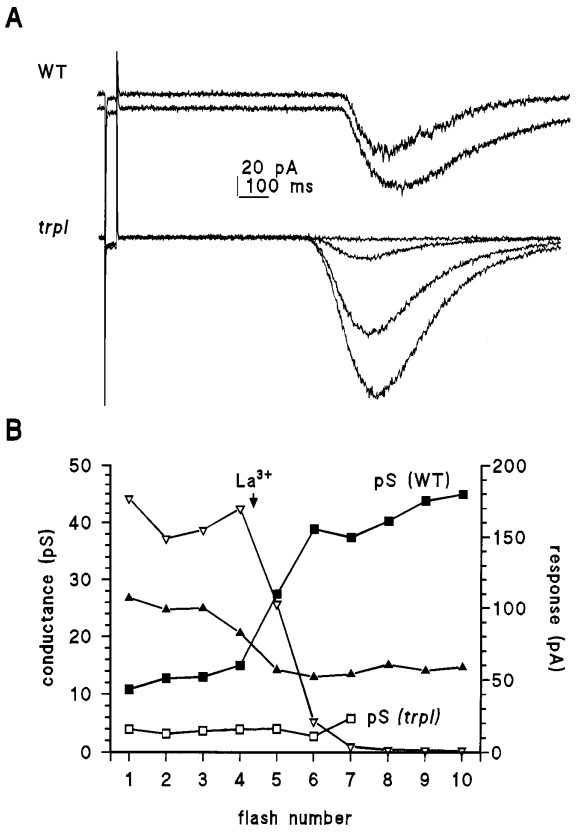

Figure 6. Lanthanum block

(A) Responses to 20 ms flashes recorded in a wild-type photoreceptor (above) and a *trpl* photoreceptor (below) immediately before and after application of La^{3+} (20 μM) from a puffer pipette placed near the recorded cell. In the wild-type cell, the smaller response is associated with relatively greater channel noise, whereas no obvious difference can be detected in the *trpl* photoreceptor, in which channel noise is uniformly low. In *trpl*, but not wild type, La^{3+} results in a complete block of the response.

(B) Peak response (triangles) and effective single channel conductance (squares) calculated from variance/mean ratio before and after La^{3+} application in wild type (closed symbols) and *trpl* (open symbols). This confirms the increase in apparent channel conductance in wild-type flies, whereas in *trpl* the effective channel conductance is small and unaffected by La^{3+}. Flashes were repeated at 8 s intervals.

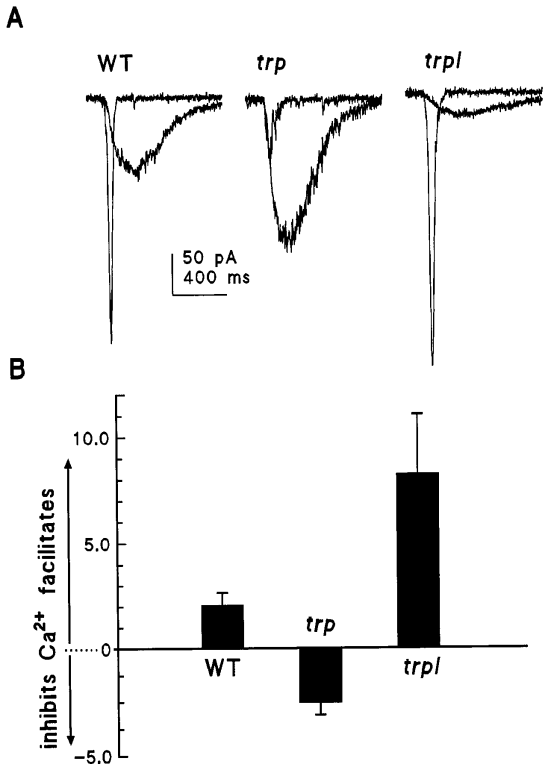

Figure 7. Differential Regulation of TRP and TRPL Channels by Ca^{2+}

(A) Each pair of traces shows responses to brief (10 ms) flashes in the presence (rapid responses) and absence (slow responses) of extracellular Ca^{2+}. The rate of rise in the *trp* mutant (i.e., TRPL channels) was unaffected by Ca^{2+}, but responses terminated much more rapidly in the presence of Ca^{2+}, resulting in an overall inhibition by Ca^{2+}. In *trpl* flies (TRP-dependent channels), Ca^{2+} greatly facilitated the rising phase. In wild type, a more modest facilitation was observed.

(B) Summary of the effect of Ca^{2+} on peak responses, indicating that compared to the situation in Ca^{2+}-free Ringer's, TRP channels (in *trpl*) are facilitated ~8-fold, whereas TRPL channels are inhibited ~2.5-fold (mean ± SD from six to eight cells in each case).

various conditions. We report a number of novel phenotypic manifestations of the *trpl* mutation, and our description of the light-sensitive conductance in the *trpl* mutant represents a detailed description of the TRP-dependent channels in situ in isolation from the TRPL channel subunits.

Basis of the Wild-Type Light-Sensitive Conductance

The data in this paper are consistent with the hypothesis that the wild-type light-induced current is mediated by at least two independent conductances, which have the properties of the channels present in the *trp* and *trpl* mutants, respectively. In each situation investigated, the property of the wild-type conductance could be quantitatively accounted for by summation of the two components isolated in the *trp* and *trpl* mutant. Specifically, (1) wild-type ionic permeabilities and effective channel conductance were intermediate between those of *trp* and *trpl*; (2) unique reversal potentials were found in both *trp* and *trpl* mutants, but not in wild type; (3) the La^{3+} block in wild type (but not *trpl*) was associated with an otherwise counterintuitive increase in effective channel conductance; and (4) effective channel conductance was independent of voltage in both *trp* and *trpl* mutants but showed a very characteristic dependence in wild type, which could be completely accounted for by the summation of the TRP and TRPL channels with the properties (conductance and E_{rev}) determined in the respective mutants (Figure 5).

Relative Contributions of TRP- and TRPL-Dependent Channels

If it is accepted that the wild-type conductance is composed of two components with the properties of TRP- and TRPL-dependent channels isolated in the respective mutants, then the data allow a number of independent estimates of the relative contribution of each component to the wild-type response.

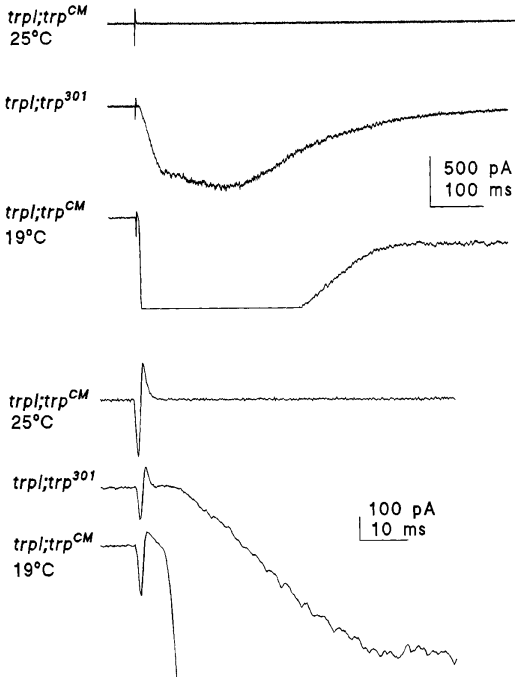

Figure 8. Responses in *trpl;trp* Double Mutants

Responses to saturating ultraviolet flashes from a high voltage (~2 ms, 300 V discharge) Xe flash gun. In both *trpl;trp^{CM}* and *trpl;trp^{301}*, the flash elicits a large biphasic early receptor current of ~100–200 pA, indicating that the cells have a near normal complement of rhodopsin. In the *trpl;trp^{301}* double mutant and in *trp;trpl^{CM}* raised at the permissive temperature of 19°C, the flash also elicits a large light-induced current (response clipped due to amplifier saturation for *trpl;trp^{CM}* raised at 19°C). However, in *trpl;trp^{CM}* raised at 25°C, there is no further response. The recordings are shown on an expanded scale below. Recordings were made under "physiological conditions" (physiological Ringer's; K gluconate electrode; holding potential, −70 mV).

First, by clamping at the reversal potentials of TRP and TRPL channels (as determined in the *trp* and *trpl* mutants), it should be possible to isolate each component in wild type, so that the relative size of the responses at the respective reversal potentials should provide a direct estimate of the relative contribution of the two channels to the light response. Interpolation from the same recordings used for the voltage dependence of noise analysis (e.g., Figure 5) lead to an estimate of 56% ± 22% TRPL- and 44% ± 22% TRP-dependent conductance (mean ± SD; n = 14; based on peak responses in wild type at mean E_{rev} in *trp* and *trpl*).

Second, the complex dependence of effective channel conductance on voltage (Figure 5) could be closely modeled on the assumption of two independent components. The data were well-fitted, assuming an equal proportion was carried by each component.

Third, on a two channel model the wild-type permeability is predicted to be the weighted average of the two components. In three cases (Ca^{2+}, Mn^{2+}, and Mg^{2+}), the wild-type results indicated a combination of ~50%–60% TRPL and ~40%–50% TRP (Table 1). For Na^{+}, a smaller proportion of TRPL was indicated; however, differences in reversal potentials between TRP and TRPL with monovalent ions were much smaller than with divalent ions, so that errors of only 1–2 mV in the estimation of E_{rev} would lead to large errors in the estimation of relative proportions of the two conductances. A significant exception was found, however, with respect to currents carried by Ba^{2+}, in which it seems that 90% of the current is carried by TRP channels. Such a discrepancy could be explained by a pharmacological effect of Ba^{2+} on open probability or single channel conductance.

Fourth, the effective single channel conductance determined by noise analysis in wild type in Ca^{2+}-free Ringer's at resting potential was 17 ± 10 pS. This would be accounted for by a 58% ± 32% contribution from TRP channels (4 pS) and a 42% ± 32% contribution from TRPL channels (35 pS).

Most of these estimates, which are almost entirely independent, give a similar result—namely, approximately equal relative contributions of TRP and TRPL in terms of total current—since the single channel conductance of TRP is ~10× less than that of TRPL, this indicates that there should be ~10× more TRP channels than TRPL channels contributing to the responses. This is consistent with a recent quantitative estimate of the amounts of TRP and TRPL protein expressed in Drosophila eyes (Xu et al., 1997).

It should be emphasized that all of these estimates refer to rather specific conditions: namely, either in Ca^{2+}-free Ringer's or around reversal potential. Although we found a similar relationship (~50:50) using a variety of independent estimates, this relation is not expected to be constant under all conditions, most notably because of major differences in the regulation of the two channels by Ca^{2+} influx. As we show here (Figure 7), the activity of TRP-dependent channels in the *trpl* mutant is initially greatly facilitated by Ca^{2+}, whereas the TRPL channels show only Ca^{2+}-dependent inactivation. Quantitatively, the difference in Ca^{2+} dependence (~20-fold increase of TRP relative to TRPL in the presence of Ca^{2+}) predicts that TRP channels should account for ~95% of the wild-type response at resting potential in the presence of Ca^{2+} and can thus explain the observation that flash responses and quantum bumps, recorded at resting potential in the *trpl* mutant, appear essentially indistinguishable from wild type in the presence of physiological Ca^{2+} (Niemeyer et al., 1996; S. R. Henderson and R. C. H., unpublished data). The physiological role of the TRPL channels remains an open question; presumably, their relative contribution will increase as the cell depolarizes, not only because of the reduced Ca^{2+} influx but also because of a voltage-dependent dependent block by Mg^{2+}, which is specific to the TRP-dependent channels (Hardie and Mojet, 1995).

Comparison with Heterologously Expressed Channels

Recently, we reported that the ionic selectivity of heterologously expressed TRPL channels, as well as a variety of other biophysical parameters, were quantitatively indistinguishable from those in the *trp^{301}* mutant, consistent with the proposal that TRPL homomultimers mediate the light-sensitive current in the *trp^{301}* mutant (Hardie

et al., 1997). However, the properties of TRP-dependent channels determined in the *trpl* mutant deviate significantly from the available data from heterologously expressed TRP channels (e.g., Vaca et al., 1994). The most striking differences concern permeability for divalent ions. For example, permeability ratios for Ba^{2+} and Mg^{2+} were reported, respectively, as ~150- and 3000-fold lower in insect Sf9 cells than in the present study (calculated from bi-ionic E_{rev} potential data of Vaca et al., 1994). Such conspicuous discrepancies make it unlikely that the same channels were being studied in the two situations. A possible explanation would be that TRP interacts with channel subunits endogenous to the expression system. Alternatively, the native TRP-dependent light-sensitive channels might incorporate an additional, as yet unidentified channel subunit. A further implication of these considerations is that it may be premature to conclude that activation of TRP-dependent channels by thapsigargin in expression studies represents the physiological route of excitation in situ.

Our results also contrast with two recent studies, which have suggested that TRP and TRPL form heteromultimers. First, Gillo et al. (1996) reported that, following coexpression of TRP and TRPL in Xenopus oocytes, depletion of Ca^{2+} stores activated a novel current with a Mg^{2+}-dependent dual inward and outward rectification. Although such rectification is reminiscent of the Drosophila wild-type light-activated conductance, as we show here this property does not require TRPL (Figure 2). Furthermore, Gillo et al. (1996) also found a current with similar rectification when TRPL was expressed alone (though now activated constitutively rather than by store depletion). Since no such rectification is seen in TRPL channels in the *trp* mutant (Figure 2; Hardie and Minke, 1994; Hardie et al., 1997), or in TRPL channels expressed in other systems (Vaca et al., 1994; Harteneck et al., 1995; Hardie et al., 1997), it seems possible that the currents observed may have been endogenous currents activated in an unknown manner by the expressed TRP and TRPL proteins.

Second, Xu et al. (1997) reported direct in vitro evidence for heteromultimeric interactions of TRP and TRPL subunits and proposed that in vivo the wild-type conductance is composed of TRP homomultimers and TRP–TRPL heteromultimers. Since we have found that the two components of the wild-type conductance are quantitatively accounted for by the conductances found in the *trp* and *trpl* mutants, respectively, this proposal would only be consistent with our in vivo analysis if TRP–TRPL heteromultimers had essentially the same properties as TRPL alone. However, the properties of the putative heteromultimer reported by Xu et al. (1997) following coexpression of TRP and TRPL in 293T cells were distinct from those of the TRPL-dependent conductance, both when compared with TRPL heterologously expressed in the same cell line and with TRPL in vivo (in the *trp* mutant or in wild type after application of La^{3+}). Conceivably, such discrepancies may also be resolved by the involvement of a third subunit; however, the possibility should also be seriously considered that although TRP and TRPL may show evidence of interaction in vitro, they do not form functional heteromultimers in vivo.

Experimental Procedures

Flies

All experiments were performed on newly eclosed (<2 hr) Drosophila melanogaster adults. The wild-type strain was white-eyed (*w*) Oregon; to isolate TRPL-dependent channels, we used *w;trp^{301}*, which is a near null mutant without detectable TRP protein on Western blots (Pollock et al., 1995). Towards the end of this study, we discovered that the *trp^{CM}* allele (Cosens and Manning, 1969) is a more effective functional null allele; however, except in the double mutant combination (*trpl;trp*), *trp^{CM}* and *trp^{P301}* appear quantitatively indistinguishable (e.g., with respect to reversal potential and channel noise). To isolate TRP-dependent channels, we used *trpl^{302},cn,bw*, a null allele kindly provided by Dr C. Zuker (La Jolla), which has a nonsense codon just prior to the transmembrane sequences (Niemeyer et al., 1996). Flies were raised at 25°C unless otherwise stated.

Electrophysiological Recording and Stimulation

Dissociated ommatidia were prepared as previously described (Hardie, 1991, 1996b). Briefly, retinae were rapidly dissected out and triturated, and the dissociated ommatidia were allowed to settle in a recording chamber on the stage of an inverted microscope (Nikon Diaphot). Whole-cell recordings were made using unsylgarded pipettes 5–10 MΩ in resistance. Series resistances were in the range 10–20 MΩ; for most measurements, series compensation of 70%–80% was applied, but for noise analysis no compensation was applied, and the clamp time constant was monitored repeatedly using 10 mV voltage pulses at the start of each sampled data trace. Series resistance errors (typically of the order of 1 mV) were calculated and corrected for in all quantitative data. Stimulation was either by a green light-emitting diode (LED) focused via the condenser, a monochromatic green light (560 nm) from a 75 W Xe lamp, or a high voltage Xe flash lamp (XF-10; Hi-Tech Scientific, UK) capable of discharging up to 385 V within 2 ms. Both Xe light sources were delivered via the fluorescent port of the microscope.

Solutions

Physiological Ringer's contained (in mM) 120 NaCl, 5 KCl, 4 $MgCl_2$, 1.5 $CaCl_2$, 10 N-Tris-(hydroxymethyl)-methyl-2-amino-ethanesulphonic acid (TES), 25 proline, and 5 alanine. For bi-ionic reversal potential measurements of monovalent ions, the only external ions present were 130 mM NaCl or LiCl (solution otherwise unchanged). Divalent ions (Ba^{2+}, Mg^{2+}, Mn^{2+}, or Ca^{2+}) were used as 10 mM solutions of the chloride salt, in the presence of 120 mM N-methyl-D-glucamine Cl (NMDG Cl), 10 TES, 25 proline, and 5 alanine. "Physiological" pipette solution contained (in mM) 140 K gluconate, 10 TES, 4 Mg ATP, 2 $MgCl_2$, and 0.4 Na GTP. For reversal potential measurements using physiological Ringer's solutions, K gluconate was replaced with 120 mM CsCl and 15 mM TEA. For bi-ionic reversal potential measurements using monovalent ions, the pipette contained 130 mM Cs gluconate and 10 mM TES. For measurements of bi-ionic reversal potentials when Ca^{2+} was the only permeant extracellular ion, it was found necessary to protect the cells from Ca^{2+} overload (due to inhibition of Na/Ca exchange). For this purpose, cells were initially bathed in a solution containing 130 NMDG Cl, 10 TES, 25 proline, and 5 alanine and recorded from using a pipette containing 130 mM Cs gluconate and 10 mM TES with 10 mM EGTA and 1 mM $CaCl_2$. Only after establishing the whole-cell configuration was the solution containing 10 mM Ca^{2+} perfused onto the cell from a wide-bored (~20 μm) puffer pipette. Although not strictly necessary, an identical procedure was followed for determination of E_{rev} of the other divalent ions as well. All solutions were buffered to a pH of 7.15. The Cs gluconate pipette solutions induced a junction potential of −12 mV; K gluconate, a potential of −10 mV; and CsCl-TEA solutions, a potential of −3 mV; these were corrected for in the data. Chemicals were obtained from Sigma.

Nonstationary Noise Analysis

Each light response was fitted with a smooth function, which was achieved by fitting 100 ms data segments (sampled at 5 kHz, Bessel filtered at 2 kHz) with fourth order polynomial functions: the fit was repeated for overlapping segments at 12.5 ms intervals and the final fit synthesised from the central 12.5 ms of each individual fit. This

fitted function was subtracted from each trace to extract the high frequency channel noise. The variance of this noise was measured in short (50 ms) overlapping segments (repeated at 12.5 ms intervals) and the mean value from the corresponding time region of the original data trace. Baseline mean and variance were determined in the dark in identical fashion during the 250 ms immediately prior to the light stimulus and subtracted to isolate the light-induced mean current and variance.

When open probability is low, the single channel current amplitude (I) underlying the macroscopic noise is given simply by variance/mean (Colquhoun and Hawkes, 1977). When this assumption holds, variance/mean is constant and independent of mean current. Variance versus mean plots of the data were essentially linear, suggesting that this assumption holds, and single channel currents (I) were therefore taken as the slopes of the variance/mean plots (in pA). For the case of more than one channel (or multiple subconductance states), the result should represent the weighted average of the different single channel currents. As described elsewhere (Hardie et al., 1997), power spectra may also be derived from such data and were indistinguishable from power spectra obtained from channel noise obtained under steady-state conditions (during either the so-called run-down current or in heterologously expressed channels). Channel conductance, γ, was calculated as a chord conductance: i.e., $\gamma = I/V$, where V (in volts) equals the holding potential minus the reversal potential; finally, a correction was made for the power estimated to have been lost by filtering of the recording bandwidth. This correction was made by comparing the integrated areas under idealized noise power spectra (based on Lorentzian fits) before and after convolving with a function describing the combined filtering characteristics of the clamp time constant (the major limiting factor), the Bessel filter (fourth order, 2 kHz), and the loss at low frequencies due to subtraction of the fitting algorithm.

Acknowledgments

This research was supported by grants from the BBSRC (INS02820) and Wellcome Trust (050444). The authors wish to thank Professors Baruch Minke, Craig Montell, and Bill Schilling for discussion and helpful comments on an earlier version of the manuscript.

Received August 4, 1997; revised November 4, 1997.

References

Clapham, D.E. (1996). TRP is cracked but is CRAC TRP? Neuron *16*, 1069–1072.

Colquhoun, D., and Hawkes, A.G. (1977). Relaxation and fluctuations of membrane currents that flow through drug-operated channels. Proc. R. Soc. Lond. [Biol.] *199*, 231–262.

Cosens, D.J., and Manning, A. (1969). Abnormal electroretinogram from a *Drosophila* mutant. Nature *224*, 285–287.

Gillo, B., Chorna, I., Cohen, H., Cook, B., Manistersky, I., Chorev, M., Arnon, A., Pollock, J.A., Selinger, Z., and Minke, B. (1996). Coexpression of Drosophila TRP and TRP-like proteins in Xenopus oocytes reconstitutes capacitative Ca^{2+} entry. Proc. Natl. Acad. Sci. USA *93*, 14146–14151.

Gomez, M.D.P., and Nasi, E. (1996). Ion permeation through light-activated channels in rhabdomeric photoreceptors: role of divalent cations. J. Gen. Physiol. *107*, 715–730.

Hardie, R.C. (1991). Whole-cell recordings of the light-induced current in *Drosophila* photoreceptors: evidence for feedback by calcium permeating the light sensitive channels. Proc. R. Soc. Lond. [Biol.] *245*, 203–210.

Hardie, R.C. (1995). Photolysis of caged Ca^{2+} facilitates and inactivates but does not directly excite light-sensitive channels in *Drosophila* photoreceptors. J. Neurosci. *15*, 889–902.

Hardie, R.C. (1996a). Setting store by calcium. Curr. Biol. *6*, 1371–1373.

Hardie, R.C. (1996b). INDO-1 measurements of absolute resting and light-induced Ca^{2+} concentration in Drosophila photoreceptors. J. Neurosci. *16*, 2924–2933.

Hardie, R.C., and Minke, B. (1992). The *trp* gene is essential for a light-activated Ca^{2+} channel in Drosophila photoreceptors. Neuron *8*, 643–651.

Hardie, R.C., and Minke, B. (1993). Novel Ca^{2+} channels underlying transduction in Drosophila photoreceptors: implications for phosphoinositide-mediated Ca^{2+} mobilization. Trends Neurosci. *16*, 371–376.

Hardie, R.C., and Minke, B. (1994). Spontaneous activation of light-sensitive channels in Drosophila photoreceptors. J. Gen. Physiol. *103*, 389–407.

Hardie, R.C., and Minke, B. (1995). Phosphoinositide-mediated phototransduction in Drosophila photoreceptors: the role of Ca^{2+} and *trp*. Cell Calcium *18*, 256–274.

Hardie, R.C., and Mojet, M.H. (1995). Magnesium-dependent block of the light-activated and *trp*-dependent conductance in *Drosophila* photoreceptors. J. Neurophysiol. *74*, 2590–2599.

Hardie, R.C., Reuss, H., Lansdell, S.J., and Millar, N.S. (1997). Functional equivalence of native light-sensitive channels in the *Drosophila* trp^{301} mutant and TRPL cation channels expressed in a stably transfected *Drosophila* cell line. Cell Calcium *21*, 431–440.

Harteneck, C., Obukhov, A.G., Zobel, A., Kalkbrenner, F., and Schultz, G. (1995). The Drosophila cation channel trpl expressed in insect Sf9 cells is stimulated by agonists of G protein–coupled receptors. FEBS Lett. *358*, 297–300.

Hille, B. (1992). Ionic channels in excitable membranes. (Sunderland, MA: Sinauer).

Hochstrate, P. (1989). Lanthanum mimicks the trp photoreceptor mutant of Drosophila in the blowfly Calliphora. J. Comp. Physiol. [A] *166*, 179–187.

Hoth, M., and Penner, R. (1993). Calcium release-activated calcium current in rat mast cells. J. Physiol. *465*, 359–386.

Lan, L., Bawden, M.J., Auld, A.M., and Barritt, G.J. (1996). Expression of Drosophila *trpl* cRNA in Xenopus laevis oocytes leads to the appearance of a Ca^{2+} channel activated by Ca^{2+} and calmodulin, and by guanosine 5′[gamma-thio]trisphosphate. Biochem. J. *316*, 793–803.

Minke, B. (1983). The *trp* is a *Drosophila* mutant sensitive to developmental temperature. J. Comp. Physiol. [A] *151*, 483–486.

Minke, B., and Selinger, Z. (1996). The roles of *trp* and calcium in regulating photoreceptor function in Drosophila. Curr. Opin. Neurobiol. *6*, 459–466.

Minke, B., Wu, C.-F., and Pak, W.L. (1975). Induction of photoreceptor noise in the dark in a Drosophila mutant. Nature *258*, 84–87.

Montell, C., and Rubin, G.M. (1989). Molecular characterization of Drosophila *trp* locus: a putative integral membrane protein required for phototransduction. Neuron *2*, 1313–1323.

Niemeyer, B.A., Suzuki, E., Scott, K., Jalink, K., and Zuker, C.S. (1996). The Drosophila light-activated conductance is composed of the two channels TRP and TRPL. Cell *85*, 651–659.

Pak, W.L., and Liddington, K.J. (1974). Fast electrical potential from a long-lived long wavelength photoproduct of fly visual pigment. J. Gen. Physiol. *63*, 740–756.

Petersen, C.C.H., Berridge, M.J., Borgese, M.F., and Bennett, D.L. (1995). Putative capacitative calcium entry channels: expression of Drosophila *trp* and evidence for the existence of vertebrate homologs. Biochem. J. *311*, 41–44.

Phillips, A.M., Bull, A., and Kelly, L.E. (1992). Identification of a Drosophila gene encoding a calmodulin-binding protein with homology to the *trp* phototransduction gene. Neuron *8*, 631–642.

Pollock, J.A., Assaf, A., Peretz, A., Nichols, C.D., Mojet, M.H., Hardie, R.C., and Minke, B. (1995). TRP, a protein essential for inositide-mediated Ca^{2+} influx is localized adjacent to the calcium stores in Drosophila photoreceptors. J. Neurosci. *15*, 3747–3760.

Ranganathan, R., Malicki, D.M., and Zuker, C.S. (1995). Signal transduction in Drosophila photoreceptors. Annu. Rev. Neurosci. *18*, 283–317.

Suss-Toby, E., Selinger, Z., and Minke, B. (1991). Lanthanum reduces the excitation efficiency in fly photoreceptors. J. Gen. Physiol. *98*, 849–868.

Vaca, L., Sinkins, W.G., Hu, Y., Kunze, D.L., and Schilling, W.P. (1994). Activation of recombinant trp by thapsigargin in Sf9 insect cells. Am. J. Physiol. [Cell Physiol.] *267*, C1501–C1505.

Wes, P.D., Chevesich, J., Jeromin, A., Rosenberg, C., Stetten, G., and Montell, C. (1995). TRPC1, a human homolog of a Drosophila store-operated channel. Proc. Natl. Acad. Sci. USA *92*, 9652–9656.

Xu, X.-Z.S., Li, H.-S., Guggino, W.B., and Montell, C. (1997). Coassembly of TRP and TRPL produces a distinct store-operated conductance. Cell *89*, 1155–1164.

Zhu, X., Jiang, M., Peyton, M., Boulay, G., Hurst, R., Stefani, E., and Birnbaumer, L. (1996). *trp*, a novel mammalian gene family essential for agonist-activated capacitative Ca^{2+} entry. Cell *85*, 661–671.

Zitt, C., Zobel, A., Obukhov, A.G., Harteneck, C., Kalkbrenner, F., Luckhoff, A., and Schultz, G. (1996). Cloning and functional expression of a human Ca^{2+}-permeable cation channel activated by calcium store depletion. Neuron *16*, 1189–1196.

Zuker, C.S. (1996). The biology of vision in Drosophila. Proc. Natl. Acad. Sci. USA *93*, 571–576.